

# Photobiomodulation at 830 nm influences diabetic wound healing *in vitro* through modulation of inflammatory cytokines

T N Mgwenya, H Abrahamse and N N Houreld

Laser Research Centre, Faculty of Health Sciences, University of Johannesburg, P.O Box 17011, Doornfontein, South Africa, 2028

E-mail: [nhoureld@uj.ac.za](mailto:nhoureld@uj.ac.za)

**Abstract.** Diabetes remains a global challenge, associated with delayed wound healing due to increased oxidative stress and pro-inflammatory cytokines. Photobiomodulation (PBM) induces wound healing through diminishing inflammation and oxidative stress and has been successfully used for healing diabetic ulcers *in vivo*. This study investigated the effects of PBM at 830 nm and a fluence of 5 J/cm<sup>2</sup> on inflammation in an *in vitro* diabetic wounded cell model. To achieve this, fibroblast cells were cultured under hyperglycaemic conditions, wounded via the central scratch, irradiated, and incubated for 24 h and 48 h. Pro-inflammatory cytokines (interleukin-6, IL-6; tumour necrosis factor-alpha, TNF- $\alpha$ ; and cyclooxygenase-2, Cox-2) were measured using ELISA. Post-PBM there were no significant changes in IL-6 and Cox-2 at both 24 and 48 h; the only significant change was the increase in TNF- $\alpha$  at 24 h. Despite TNF- $\alpha$  and Cox-2 being pro-inflammatory cytokines, they have been found to promote healing in the early stages of wound healing. PBM at 830 nm with 5 J/cm<sup>2</sup> does not appear to influence inflammation in a diabetic wounded cell model as measured by IL-6 and Cox-2.

## 1. Introduction

Diabetes Mellitus (DM) remains a global health concern. According to the International Diabetes Federation (IDF), 537 million adults between the ages of 20 and 79 were living with diabetes worldwide in 2021, and this is predicted to reach 643 million by 2030 and 783 million by 2045 [1]. DM is linked to complicated wound healing. Diabetic foot ulcers (DFUs) are common in patients living with type-2 DM. Infection, ulcer formation, and deep-tissue necrosis are the most common complications that contribute to chronic wounds in type-2 DM patients due to the combination of neuropathy and various degrees of peripheral vasculopathy [2]. A high glucose environment causes difficulty in wound healing. Diabetic wounds are often associated with increased inflammation, reduced fibroblasts (essential cells for wound repair) and cellular proliferation, and decreased cytokine and growth factor production [3].

Current treatments for chronic wounds remain ineffective to some degree, with a high rate of failure and relapse. Only a 50% healing rate is achieved [4]. This demonstrates the need to research and develop new therapies, including photobiomodulation (PBM), and a better understanding of their underlying cellular and molecular effects on diabetic wound healing. Several studies have been conducted on PBM, and many of these have demonstrated the benefits of PBM on wound healing. However, the accepted working parameters of PBM (wavelength/s, fluencies, and duration) on wound healing have not been adequately optimized. PBM is typically used in the red and near-infrared (NIR) electromagnetic

spectrum, with most *in vitro* studies conducted in the red spectrum [5]. There are few reports on PBM at 830 nm as an approach to enhance wound healing in diabetic patients. This study aimed to investigate the effect of PBM at 830 nm at a fluence of 5 J/cm<sup>2</sup> on inflammation in a diabetic wounded fibroblast cell model.

## 2. Materials and methods

### 2.1. Cell culture

A human skin fibroblast cell line, commercially purchased from the American Type Culture Collection (WS1, ATCC® CRL-1502™) was used in this study. The cell line was cultured under standard conditions in minimum essential medium (MEM) supplemented with 1 mM sodium pyruvate, 0.1 mM non-essential amino acids (NEAA), 2 mM L-glutamine, 1% penicillin-streptomycin, 1% amphotericin B, and 10% fetal bovine albumin (FBS) and incubated at 37°C, 5% CO<sub>2</sub> and a humidity of 85%.

WS1 human fibroblast cells were continuously grown under hyperglycemic conditions using supplemented MEM with an additional 17 mM D-glucose [6]. MEM already has a basal glucose concentration of 5.6 mM, thus cells were grown for several passages before experiments in 22.6 mM D-glucose. For experiments, cells were seeded at a density of  $6 \times 10^5$  into 3.4 cm diameter culture dishes for 24 h to allow for attachment. To achieve a diabetic wounded model, a ‘wound’ was created by the central scratch assay [7, 8]. A cell-free zone (‘wound’) with cells on either side and a wound margin was created in the cell monolayer by scraping the confluent cell layer with a 1 mL sterile pipette.

### 2.2. Laser irradiation

Thirty minutes post ‘wounding’, cells were irradiated using a laser in the Laser Research Centre (LRC) laboratory, set up by the Council for Scientific and Industrial Research (CSIR)/National Laser Centre (NLC), at an emission wavelength of 830 nm. Laser irradiation at 830 nm and a fluence of 5 J/cm<sup>2</sup> stimulates WS1 cells [9]. For experiments, a power meter (FieldMate) was used to measure the laser power output (mW) before irradiating the cells. The value obtained was used to determine the exposure duration (s) by calculating the output power density (mW/cm<sup>2</sup>). Table 1 provides the laser parameters used in this study.

**Table 1.** Laser parameters.

Variables	Diode Laser
Wavelength (nm)	830
Wave emission	Continuous wave
Power output (mW)	106
Power output density (mW/cm <sup>2</sup> )	11.68
Spot size (cm <sup>2</sup> )	9.1
Irradiation time (s)	428
Fluence (J/cm <sup>2</sup> )	5
Energy (J)	45.4

WS1 human fibroblast cells were irradiated via fiber optics from above with the culture dish lid off and in the dark to prevent any light interference. Non-irradiated cells (0 J/cm<sup>2</sup>) served as controls. The laser irradiation effects were determined by looking at various cellular responses analyzed after 24 h and 48 h incubation. This was evaluated by studying the morphology and migration of cells and conducting biochemical assays to determine levels of inflammatory cytokines.

### 2.3. Morphological changes and migration rate

Morphological changes were determined using inverted light microscopy (Olympus CKX41), and images were taken using analysis getIT software. The cellular migration towards the center of the central scratch was determined at 24 h and 48 h post-irradiation. This was achieved by measuring the wound gap width ( $\mu\text{m}$ ) between the wound margins of the cell free zone. The rate of migration is expressed in percentage using the equation:

$$(A_{t_{0h}} - A_{t_{\text{time}}})/A_{t_{0h}} \times 100,$$

where  $A_{t_{0h}}$  is the distance between the edges of the central scratch at 0 h, and  $A_{t_{\text{time}}}$  is the successive distance between the edges of the central scratch at various time points [10].

### 2.4. Quantitative analysis of inflammatory cytokines

The Enzyme-Linked Immunosorbent Assay (ELISA) was used to detect levels of the inflammatory markers (Cox-2, IL-6, and TNF- $\alpha$ ) released by cells into the surrounding culture media. The human Cox-2 ELISA kit (Sigma-Aldrich, RAB1034), human TNF- $\alpha$  ELISA kit (Sigma-Aldrich, RAB0476), and human IL-6 ELISA kit (Sigma-Aldrich, RAB0306) were used to determine the levels of the three inflammatory cytokines as per the manufacturer's instructions. All reagents and samples were brought to room temperature (18–25°C) to thaw before use. The standards and culture media samples (100  $\mu\text{L}$ ) were added in duplicate to their appropriate wells on a coated 96-well microplate, covered with microplate sealer, and incubated at 4°C with gentle shaking overnight.

Following overnight incubation, the standards and samples were discarded, and the plates washed four times with sample wash buffer (diluted 5-fold in distilled water). A biotinylated detection antibody (100  $\mu\text{L}$  diluted 80-fold in assay diluent buffer) was added to each well, and plates were incubated for 1 h at room temperature with gentle shaking. The wash step was repeated as described previously, and freshly prepared horseradish peroxidase (HRP)-Streptavidin solution (diluted 600-fold in assay diluent buffer) was added (100  $\mu\text{L}$ ) to each well and incubated for a further 45 min at room temperature with gentle shaking. The wash step was repeated and ELISA colorimetric 3,3',5,5'-tetramethylbenzidine (TMB) reagent (100  $\mu\text{L}$ ) added to each well. The plates were incubated for 30 min in the dark with gentle shaking at room temperature. To each well, 50  $\mu\text{L}$  of stop solution was added and absorbance was read immediately at 450 nm using a multiplate reader (Perkin Elmer, Victor<sup>3</sup> 1420).

### 2.5. Statistical analysis

Experiments were conducted in triplicate ( $n = 3$ ), and assays in duplicate. SigmaPlot version 12.0 was used for statistical analysis and to create graphs showing the mean and standard error of the biochemical assay conducted. To identify statistical variances between the experimental and control groups, the student t-test was applied. When values were less than 0.05, the results were deemed significant ( $P < 0.001^{***}$ ,  $P < 0.01^{**}$ , and  $P < 0.05^*$ ).

## 3. Results and discussion

### 3.1. Morphological changes and migration rate

Skin can regenerate and create a collagenous scar to replace lost or damaged tissue. Fibroblast cells follow the patterns of migration as a loosely connected population. Figure 1 depicts typical fibroblast morphology, with cells appearing long and spindle shaped. At 0 h non-irradiated (0 J/cm<sup>2</sup>) and irradiated (5 J/cm<sup>2</sup>) cells did not show morphological changes. At 24 h both models showed changes in growth direction and cellular projections towards the central scratch, however the irradiated cell model started to show increased cell confluency with fewer gaps compared to non-irradiated cells. At 48 h the central scratch was completely closed with increased cell confluence in irradiated cells, while open gaps were still visible in the control cells. The irradiated DW model at 48 h showed an increase in cell orientation and cell movement across the central scratch when compared to all other time intervals.

The migration rate of irradiated cells was increased as compared to their controls across all time intervals (figure 2). At 24 h (figure 2a), a significant ( $P < 0.001$ ) increase in cell migration rate was noted in irradiated cells compared to non-irradiated cells. The migration rate in irradiated cells was 75% as compared to 49% in control cells. Although not significant ( $P = 0.124$ ), at 48 h irradiated cells showed a migration rate of 100% compared to non-irradiated cells which were at 95 % migration rate (figure 2b).

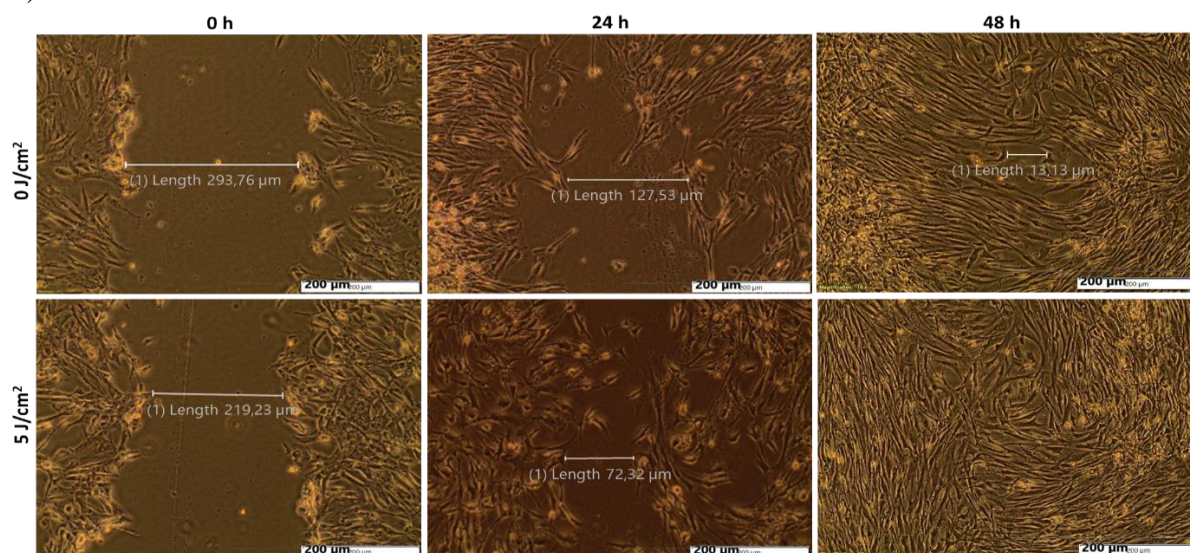


**Figure 2.** Morphological changes and cellular migration of diabetic wounded (DW) cell models post-irradiation captured at 200x magnification. Non-irradiated cells showed no significant morphological changes while irradiated cells showed an increase in migration and projection towards the central scratch, with increased cell movement at 48 h.

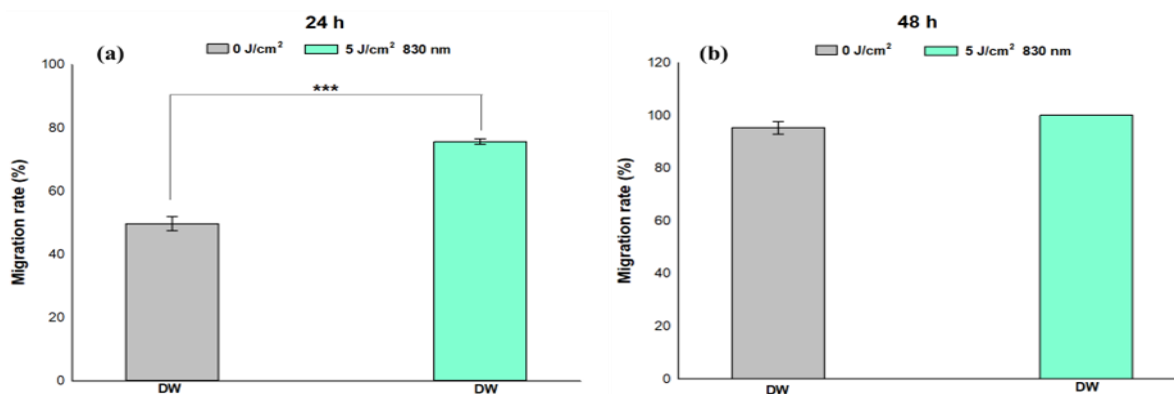


**Figure 1.** Migration rate (%) of diabetic wounded (DW) cell models. Cells showed a higher migration rate at 24 h in irradiated cells compared to non-irradiated cells. Statistical significance is presented as \*\*\* $P < 0.01$  ( $\pm$ SEM).

### 3.2. Quantitative analysis of inflammatory cytokines

ELISA was used to quantitatively measure the levels of human Cox-2, human IL-6, and human TNF- $\alpha$ . There were no significant changes in Cox-2 at 24 h ( $P = 0.642$ ) and 48 h ( $P = 0.137$ ) post-irradiation (figure 3a and b). Despite being a pro-inflammatory cytokine, Cox-2 has been found to promote healing in the early stages of wound healing [11, 12], and the Cox-2 pathway is an integral component of inflammation. Cox-2 is also thought to be an immediate gene product that can be produced quickly but

only temporarily [13]. IL-6 levels in irradiated cells initially increased ( $P = 0.842$ ) at 24 h, but this increase was not statistically significant (figure 3c). Although not statistically significant ( $P = 0.680$ ), the levels of IL-6 decreased at 48 h (figure 3d).

TNF- $\alpha$  levels were initially increased in irradiated DW cells at 24 h ( $P < 0.05$ ), however, these levels decreased at 48 h, but the difference was not significant ( $P = 0.541$ ) (figures 3e and f). Like Cox-2, TNF- $\alpha$  is a pro-inflammatory cytokine that has been found to promote healing in the early stages of wound healing [14]. A similar study conducted by our research group on WS1 human fibroblast cells at a wavelength of 660 nm with a fluence of 5 J/cm<sup>2</sup> also found a decrease in TNF- $\alpha$  levels in diabetic wounded groups at 48 h post-irradiation [14]. TNF- $\alpha$  is released by cells like endothelial cells, keratinocytes, and fibroblasts in the injured area immediately when an injury occurs to promote healing [15], which could explain the rise in TNF- $\alpha$  levels observed at 24 h.

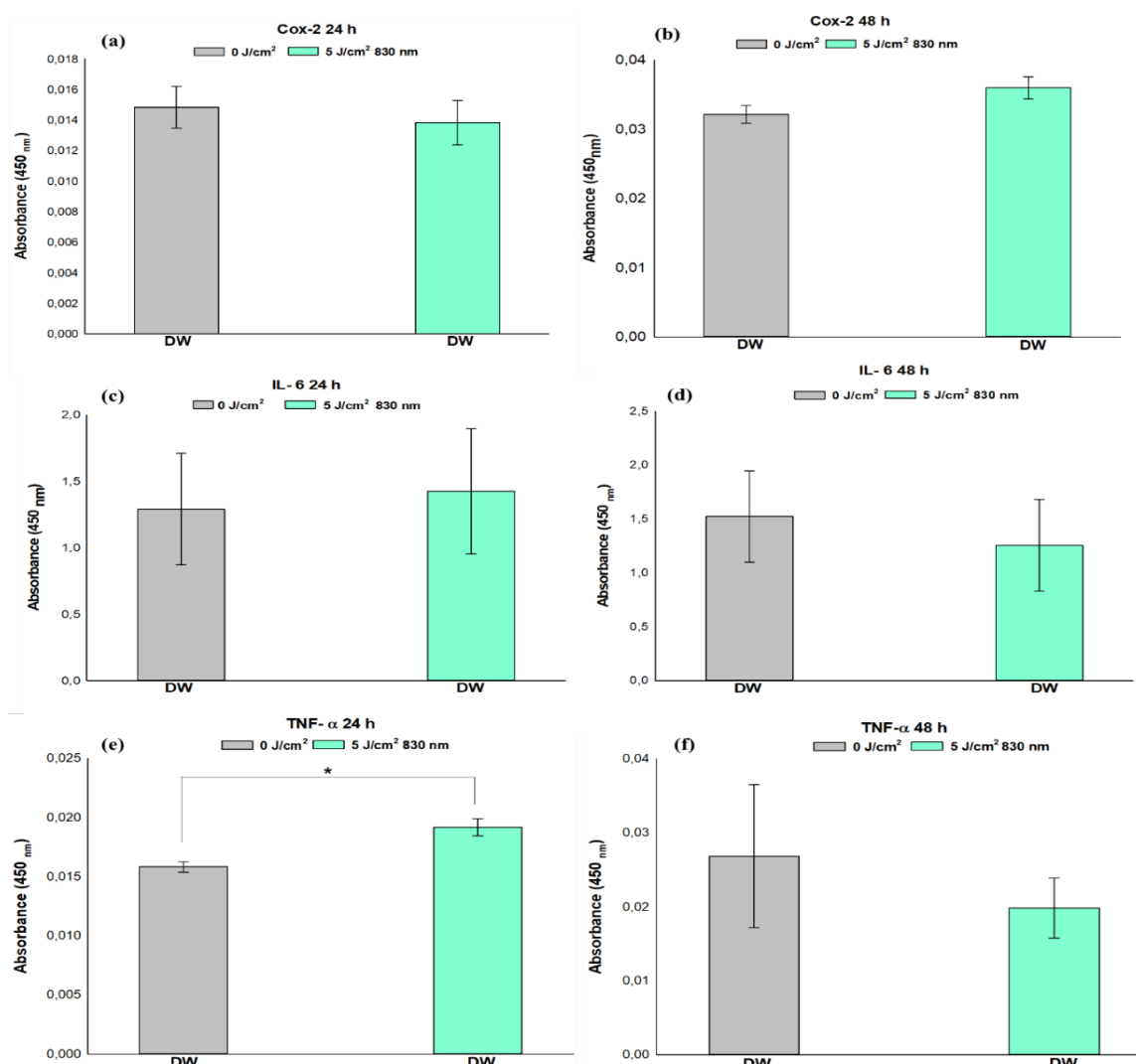


**Figure 3.** Post-irradiation analysis of the inflammatory cytokines human Cox-2, human IL-6, and human TNF- $\alpha$  in a diabetic wounded (DW) cell model at 24 h and 48 h. Non-irradiated samples served as controls. Statistical significance is presented as \* $P < 0.05$  ( $\pm$ SEM).

The creation of extracellular matrix proteins and matrix metalloproteinase, essential for the repair of injured tissues, as well as the activity of fibroblasts, vascular endothelial cells, and keratinocytes are

predominantly regulated by elevated TNF- $\alpha$  levels [15]. Additionally, during the inflammatory phase, the primary cellular sources of TNF- $\alpha$  are converted into recruited neutrophils and macrophages, and this process results in a positive recruitment boost for extending the inflammatory responses [15]. This is supported by the decreased TNF- $\alpha$  levels seen at 48 h in the current study, which is also supported by the wound closing observed in the morphological and migration studies. Although our current study was conducted *in vitro*, the results obtained are similar to the *in vivo* study by Ritsu *et al* [15] which used a mouse model with full-thickness skin wounds to examine the role of TNF- $\alpha$  in the early process of wound healing. TNF- $\alpha$  was detected shortly after the creation of the wound, increased after the first few hours, peaked in 24 h, and then decreased to the basal level.

#### 4. Conclusion

The study observed migratory effects on the DW cell model exerted by the administration of PBM at 830 nm with a fluence of 5 J/cm<sup>2</sup>. This was observed in the irradiated diabetic wounded model as they showed more cell presence in the central scratch and a higher migration rate. PBM at 830 nm with 5 J/cm<sup>2</sup> had no effect on Cox-2 and IL-6 in diabetic wounded cells *in vitro*. PBM may exert healing by stimulating the early phases of wound healing by increasing TNF- $\alpha$  levels, which decreases with the passage of time.

#### Acknowledgments

This work is based on the research supported by the South African Research Chairs Initiative of the Department of Science and Technology (DST) and National Research Foundation (NRF) of South Africa (Grant No 98337), the NRF (Grant No 129327), as well as grants received from the University of Johannesburg research council (URC), and the Council for Scientific and Industrial Research (CSIR) /National Laser Centre (NLC) Laser Rental Pool Program.

#### References

- [1] International Diabetes Federation, IDF 2021 Atlas, 10<sup>th</sup> edition, available from <https://diabetesatlas.org/> Accessed on 16/08/22
- [2] Baig M S, Banu A, Zehravi M, Rana R, Burle S S, Khan S L, Islam F, Siddiqui F A, Massoud E E S, Rahman M H and Cavalu S 2022 *Life* **12** doi: 10.3390/life12071054
- [3] Patel S, Srivastava S, Singh M R and Singh D 2019 *Biomed. Pharmacother.* 112 108615
- [4] Frykberg R G and Banks J 2015 *Adv. Wound Care* **4** 560-82
- [5] Tsai S R and Hamblin M R 2017 *J. Photochem Photobiol B* **170** 197-207
- [6] Houreld N, Sekhejane P R and Abrahamse H 2010 *Proc. Int. Conf. on WALT (Norway)* **1** (Bologna/ ScienceMED) 23-26
- [7] Liang C C, Park A Y and Guan J L 2007 *Nat. Protoc.* **2** 329-33
- [8] Houreld N and Abrahamse H. 2010. *Diabetes Technol Ther.* **12** 971-78
- [9] Houreld N and Abrahamse H 2008 *Lasers Med Sci.* **23** 11-18
- [10] Wilgus T A, Bergdall V K, Tober K L, Hill K J, Mitra S, Flavahan N A and Oberyszyn T M 2004 *Am J. Pathol.* **165** 753-61
- [11] Szweda M, Rychlik A, Babińska I and Pomianowski A 2019 *J. Vet Res.* **63** 215-24
- [12] Piipponen M, Li D and Landén N X 2020 *Int J Mol Sci.* **21** 8790 doi: 10.3390/ijms21228790
- [13] Ashcroft G S, Jeong M J, Ashworth JJ, Hardman M and Jin W 2013 *Wound Repair Regen.* **20** 38-49
- [14] Shaikh-Kader A, Houreld N N, Rajendran N K and Abrahamse H 2021 *Oxid. Med. Cell. Longev.* **2021** doi:10.1155/2021/6667812
- [15] Ritsu M, Kawakami K, Kanno E, Tanno H, Ishii K, Imai Y, Maruyama R and Tachi M 2017 *J. Dermatology Dermatologic Surg.* **21** 14-19